

# Computational study of multivessel coronary disease: haemodynamic significance of stenoses in simulation

S.S. Simakov<sup>1 a,b</sup>, T.M. Gamilov<sup>a,b</sup>, Ph.Yu.Kopylov<sup>c,b</sup>, Yu.V.Vassilevski<sup>a,b</sup>

<sup>a</sup> Moscow Institute of Physics and Technology  
141700, 9 Institutskii Lane, Dolgoprudny, Russia

<sup>b</sup> Institute of Numerical Mathematics RAS  
119333, 8 Gubkina st., Moscow, Russia

<sup>c</sup> I.M. Sechenov First Moscow State Medical University  
119991, 2-4 Bolshaya Pirogovskaya st., Moscow, Russia

## Abstract

We use a mathematical model of one-dimensional blood flow in a network of blood vessels for *in silico* evaluation of haemodynamic significance of stenoses during the multivessel coronary disease. We address two cases: (1) two stenosed vessels with different diameters and with the same degree of occlusion, (2) two serial stenoses in the same vessel. We show that two criteria for the evaluation of haemodynamic significance, the degree of the stenosis and the fractional flow reserve (FFR), may give contradictory indications for a surgical intervention. We also show that FFR computation originally proposed for a single stenosis should be modified in the case of multivessel stenotic disease.

Keywords: fractional flow reserve, mathematical modelling, computational haemodynamics.

## 1. Introduction

The coronary heart disease is the main cause of death of working age patients in Russia. Contemporary treatment of the disease requires a detailed assessment of coronary blood flow. The fractional flow reserve (FFR) is the golden standard for decision-making in coronary revascularization since it is shown to be the independent prognosticator in patients with the coronary artery disease [4]. FFR is measured during the invasive coronary angiography. Multiple lesions in coronary vasculature fuzzify the FFR notion and thus complicate surgical decision-making in coronary revascularization. *In silico* evaluation of haemodynamic significance of stenoses can greatly facilitate angiosurgical decision-making and individualize the therapy. Standard coronary computed tomography (CT) data sets provide patient-specific haemodynamic simulation on the basis of physiological models, computational fluid dynamics and quantitative anatomic models. Computational patient-specific model of coronary haemodynamics helps to extend the FFR notion to the case of multiple occlusions and thus to facilitate angiosurgical decision-making.

We have developed a mathematical model of blood flow in coronary vessels based on

---

<sup>1</sup>Corresponding author. E-mail: [simakov.ss@mipt.ru](mailto:simakov.ss@mipt.ru)

patient-specific data [3,2,7]. Using this model we evaluated FFR *in silico* for two patients with multiple lesions of coronary vessels [3], and performed numerical study of FFR sensitivity to the stroke volume variability [3], to the heart rate variability and joint heart rate and stroke volume variability [7]. In this work we present the numerical study of FFR for the following cases: (1) two stenosed vessels with different diameters and with the same degree of stenosis, (2) two serial stenoses in the same vessel. These results clarify the role of FFR in the assessment of haemodynamic significance of the stenoses during the multivessel stenotic disease.

## 2. Methods

**Mathematical model of the blood flow.** We sketch briefly the mathematical model of one-dimensional (1D) blood flow in a network of blood vessels [6]. For a detailed description we refer to [3,6] and references therein. The flow in a single linear vessel or its segment is described by mass and momentum balance equations

$$\partial S_k / \partial t + \partial (S_k u_k) / \partial x = 0, \quad (1)$$

$$\partial u_k / \partial t + \partial (u_k^2 / 2 + p_k / \rho) / \partial x = f_{fr}, \quad (2)$$

where  $k$  is the index of the vessel,  $t$  is the time,  $x$  is the coordinate along the vessel,  $\rho$  is the blood density,  $S_k(t, x)$  is the vessel cross-section area,  $p_k$  is the blood pressure,  $u_k(t, x)$  is the linear velocity averaged over the cross-section,  $f_{fr}$  is the friction force. Elastic properties of the vessel wall material are described by function

$$p_k(S_k) - p_{*k} = \rho_m c_k^2 f(S_k), \quad (3)$$

where  $f(S_k)$  is a monotone S-like function,  $p_{*k}$  is the external pressure due to myocard contraction,  $\rho_m$  is the density of the vessel's wall material,  $c_k$  is the velocity of small disturbances propagation in the vessel wall. The values  $c_k$  are set according to [5].

**Boundary conditions.** At the input to the arterial part of the network, the blood flow is given by the flux

$$u(t, 0) S(t, 0) = Q_{in}(t), \quad (4)$$

where  $Q_{in}(t)$  is the heart ejection profile. At the output from the venous part the pressure is set to  $8mmHg$ . At each nodal junction of  $M$  vessels with indexes  $k = k_1, k_2, \dots, k_M$ , we impose the mass conservation and the total pressure conservation in the form

$$\frac{u_{k_i}^2}{2} + \frac{p_{k_i}}{\rho} = \frac{u_{k_j}^2}{2} + \frac{p_{k_j}}{\rho}, i, j = 1 \dots M, i \neq j. \quad (5)$$

The nodes of arterial-venous junctions are imitated by short rigid tubes with increased hydraulic resistance where the Poiseuille pressure drop condition is postulated:

$$P_k - P_{node} = \varepsilon_k R_k S_k u_k, k = k_1, k_2, \dots, k_M. \quad (6)$$

Here  $R_k$  is the hydraulic resistance of the tube,  $\varepsilon_k = +1$  for incoming and  $\varepsilon_k = -1$  for outgoing vessel,  $P_{node}$  is the pressure in the node.

**Vascular network structure.** The 1D structure (Fig.1(3)) of the coronary arteries network is taken from [3]. The structure was extracted and identified from patient-specific data. Fig.1 represents the stages of data processing: (1) 3D segmentation, (2) centerlines extraction, (3) generation of a 3D graph with straight edges applicable for 1D haemodynamics simulations (see [2,7] for more details). The venous part is constructed on the basis of the same 1D structure by modification of functional parameters according to [3].

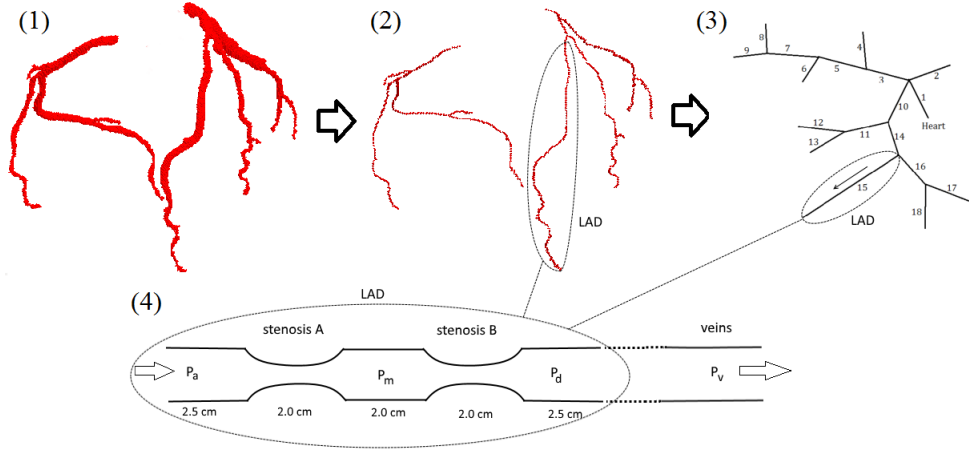


**Figure 1. Coronary arteries network reconstruction. (1) 3D segmentation of CT scans, (2) centerlines extraction, (3) 1D network (3D graph with straight edges), (4) scheme of two serial stenoses.**

**FFR evaluation.** FFR is measured during the maximum possible hyperemia caused by vasodilator administration. In the numerical model the hyperemia is simulated by a reduction of the peripheral resistance in coronary arterio-venous junctions. The values of  $R_k$  are set to  $40kBa \cdot s/cm^3$  (instead of the normal value  $200kBa \cdot s/cm^3$ ).

In the case of single stenosis, FFR is defined conventionally as the ratio of the average pressure distal to the stenosis ( $P_{dist}$ ) and the average aortic pressure ( $P_{aor}$ )

$$FFR = \frac{\overline{P}_{dist}}{\overline{P}_{aor}} \quad (7)$$

measured during the maximum possible hyperemia [8].

In the case of several serial stenoses, formula (7) may give deceiving results due to interaction between the stenoses. We adopt the definition of haemodynamic significance of every stenosis in the consecutive multivessel stenotic disease [1] to the case of the stenotic configuration shown in Fig. 1(4)

$$FFR_A^{pred} = \frac{P_d - (P_m/P_a)P_v}{P_a - P_m + P_d - P_v}, \quad FFR_B^{pred} = 1 - \frac{(P_a - P_v)(P_m - P_d)}{P_a(P_m - P_v)}, \quad (8)$$

where  $P_a, P_d, P_m, P_v$  are average pressures at the appropriate locations. We compare  $FFR_A^{pred}$ ,

$FFR_B^{pred}$  with the straightforward usage of  $FFR$  from (7) under different degrees of the stenoses  $\lambda = \left(1 - \frac{S_{st}}{S}\right)100\%$ , where  $S_{st}$  denotes the minimal area of the lumen.

### 3. Results

In the first series of numerical experiments we compare FFR (7) in vessels with different diameters and with the same degree of the single stenosis  $\lambda$ . The stenosis is located in the middle of the left anterior descending artery (LAD) (vessel 15 in Fig. 1(3)). We consider two values of the LAD diameter ( $d_{LAD}$ ),  $2mm$  and  $3mm$ . FFR is calculated for different degrees of the stenosis  $\lambda$  in the range from  $50\%$  up to  $99\%$ . Computed FFR in Fig. 2 clearly shows that different LAD with the same degree of the stenosis may have different FFR values. This is the basis for sometimes contradictory indications to surgical intervention produced by values of  $\lambda$  and FFR. Indeed, when the degree of the stenosis  $\lambda$  is used for decision-making, the cases with  $\lambda > 70\%$  should undergo stenting procedure [4]. On the other hand, FFR-based decision-making appoints a surgical intervention in cases with  $FFR < 0.75$ , whereas decision in the group of patients with  $0.75 < FFR < 0.8$  is ambiguous. The surgery-indication boundaries are shown in Fig. 2 by the dashed horizontal and vertical lines. In particular, for LAD with  $d_{LAD} = 2mm$  surgical treatment is FFR-indicated or probably indicated ( $FFR < 0.8$ ) even if the degree of the stenosis lies in the range  $57\% < \lambda < 70\%$  (curve 2 from  $a$  to  $b$ ). On the contrary, for LAD with  $d_{LAD} = 3mm$  surgical treatment is not FFR-indicated or probably not indicated ( $FFR > 0.75$ ) even if the degree of the stenosis lies in the range  $70\% < \lambda < 83\%$  (curve 1 from  $b$  to  $c$ ).

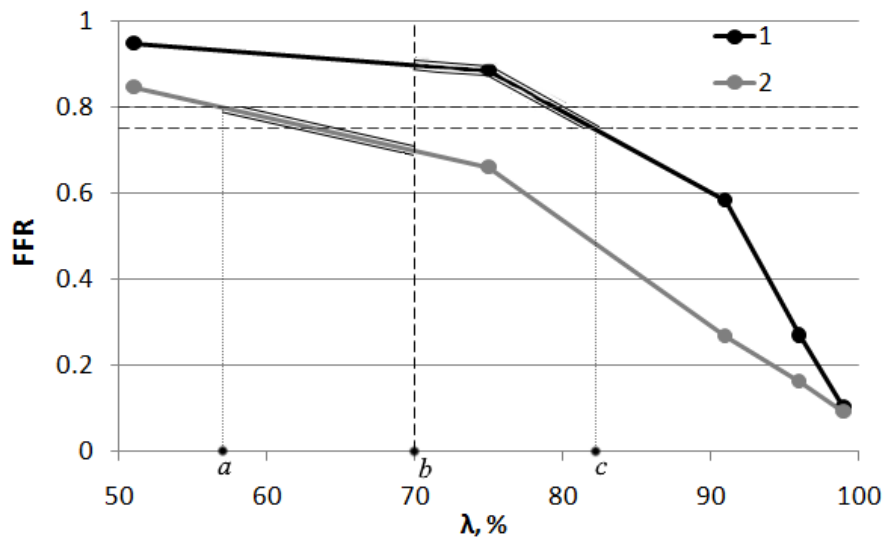


**Figure 2.** Comparison of FFR (7) for single stenosis of the same degree  $\lambda$  in LAD. Curve 1 corresponds to LAD with  $d_{LAD} = 3mm$ , curve 2 corresponds to LAD with  $d_{LAD} = 2mm$ .

In the second series of numerical experiments we consider the case of two serial stenoses in

LAD. Configuration and notation of the stenoses are shown in Fig. 1(4). The degree of the stenosis A is fixed ( $\lambda_A = 96\%$ ) and the degree of the stenosis B ( $\lambda_B$ ) is varied from 50% up to 99%,  $d_{LAD} = 2mm$ . The values of  $FFR_A$  and  $FFR_B$  are calculated by (7), (8) and compared in Fig. 3.

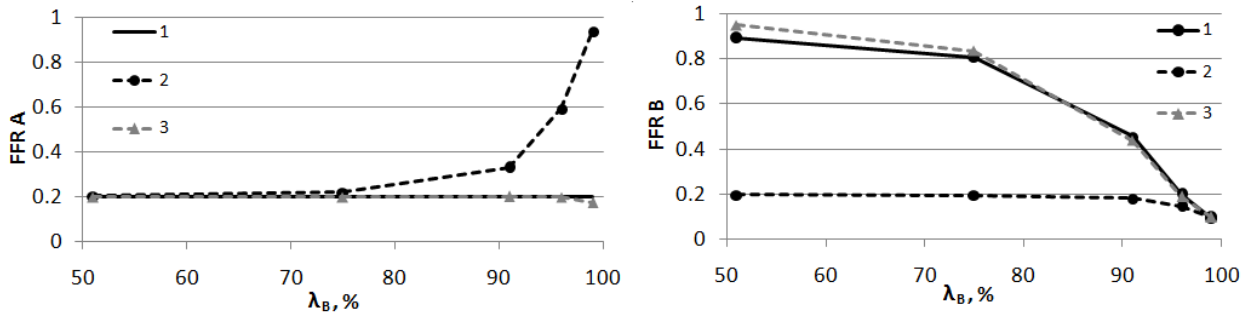


**Figure 3.** Comparison of FFR for two serial stenoses calculated by (7) and (8) during  $\lambda_B$  variations. Left: FFR at stenosis A during variation of  $\lambda_B$ , curve 1 shows  $FFR_A$  for  $\lambda_B = 0\%$  (single stenosis A), curve 2 shows  $FFR_A$  (7), curve 3 shows  $FFR_A$  (8); Right: FFR at stenosis B during variation of  $\lambda_B$ ; curve 1 shows  $FFR_B$  for  $\lambda_A = 0\%$  (single stenosis B), curve 2 shows  $FFR_B$  (7), curve 3 shows  $FFR_B$  (8).

Curves 1 and 3 in Fig. 3 demonstrate that FFR calculated by (8) for both stenoses is almost the same as FFR calculated by (7) during the absence of the other stenosis. This justifies, at least theoretically, the usability of (8) in endovascular monitoring of haemodynamic significance for each of multiple lesions of coronary vessels. On the other hand, the straightforward usage of (7) may give incorrect results (curves 2): (1) stenosis A computed by (7) tends to be haemodynamically insignificant as  $\lambda_B$  increases whereas (2) stenosis B computed by (7) is haemodynamically significant even for low values of  $\lambda_B$ . The reason for (1) is as follows: the increase of  $\lambda_B$  causes the increase of hydraulic resistance of B and the increase of  $P_m$ ; therefore, the difference between  $P_a$  and  $P_m$  reduces. The reason for (2) is the impact of substantial pressure drop due to stenosis A which is not taken into account in (7).

## 4. Conclusions

Based on the numerical haemodynamic model we showed that the degree of the stenosis  $\lambda$  is not the reliable criterion for evaluation of haemodynamic significance even of a single stenosis: it may result in substantial underestimation or overestimation of the specific case. FFR-based estimation is the more reliable measure of haemodynamic significance [4]. In the case of the multivessel coronary disease, FFR estimate provides the personalized tool for measuring haemodynamic significance of every stenosis. However, the method should be refined further to account stenoses localizations.

## 5. Acknowledgements

The work was supported by Russian Science Foundation grant No. 14-31-00024. The authors acknowledge the staff of I.M.Sechenov First Moscow State Medical University and especially N.Gagarina, E.Fominykh and A.Dzyundzya for patient-specific data. We also acknowledge help of Roman Pryamonosov in preparation of 1D structure of the patient-specific coronary network.

## References

- [1] B. De Bruyne, N.H.J. Pijls, G.R. Heyndrickx, D. Hodeige, R. Kirkeeide, K.L. Gould, Pressure-derived fractional flow reserve to assess serial epicardial stenoses: Theoretical basis and animal validation, *Circulation*, 2000, **(15)**, 1840–1847.
- [2] A.Danilov, Yu.Ivanov, R.Pryamonosov, Yu.Vassilevski. Methods of graph network reconstruction in personalized medicine. *Int.J.Numer.Meth.Biomed. Engng.*, e02754, 2016
- [3] T.M. Gamilov, Ph.Yu. Kopylov, R.A. Pryamonosov, S.S. Simakov Virtual fractional flow reserve assesment in patient-specific coronary networks by 1D hemodynamic model, *Rus. J. Num. Anal. Math. Mod.*, 2015, **(5)**, 269БЂ–276.
- [4] F.Y. Kopylov, A.A. Bykova, Y.V. Vassilevski, S.S. Simakov, Role of measurement of fractional flow reserve in coronary artery atherosclerosis, *Terapevt. Arkh.*, 2015, **(9)**, 106–113.
- [5] R. Sala, C. Rossel, P. Encinas, P. Lahiguera, Continuum of pulse wave velocity from young elite athletes to uncontrolled older patients with resistant hypertension, *J. Hyperten.*, 2010, , 19.216.
- [6] S.S. Simakov, A.S. Kholodov, Computational study of oxygen concentration in human blood under low frequency disturbances. *Math. Mod. Comp. Sim.*, 2009, **(2)**, 283–295.
- [7] Yu.V. Vassilevski, A.A. Danilov, T.M. Gamilov, Yu.A. Ivanov, R.A. Pryamonosov, S.S. Simakov. Patient-specific anatomical models in human physiology, *Rus. J. Num. Anal. Math. Mod.*, 2015, **(3)**, 185БЂ–201.
- [8] C.K. Zarins, C.A. Taylor, J.K. Min, Computed fractional flow reserve (FFTCT) derived from coronary CT angiography *J. Cardiovasc. Trans. Res.*, 2013, **(5)**, 708–714.

$\lambda$	1	2
,		
%		
	510.850.95	
	750.660.88	
	910.270.58	
	960.160.27	
	990.090.10	

**Table 1. Data for Fig. 2.**

$\lambda_B$	1	2	3
,			
%			
	510.200.210.20		
	750.200.220.20		
	910.200.330.20		
	960.200.590.20		
	990.200.940.17		

**Table 2. Data for Fig. 3, left.**

$\lambda_B$	1	2	3
,			
%			
	510.890.200.95		
	750.810.200.83		
	910.460.180.44		
	960.200.150.19		
	990.100.100.10		

**Table 3. Data for Fig. 3, right.**